Supporting Information

Constructing 3D Interconnected Fe@Graphitic Carbon Structure for Highly Efficient Microwave Absorber

*Sifan Zeng[1, 2,‡], Yu Yao [3,‡], Wanlin Feng[1], Haibin Zhang[1, *], Shuming Peng[1, 2, *]*

[1] Innovation Research Team for Advanced Ceramics, Institute of Nuclear Physics and Chemistry, China Academy of Engineering Physics, Mianyang, Sichuan, 621900, China. E-mail: hbzhang@caep.cn, pengshuming@caep.cn

[2] Department of Engineering and Applied Physics, University of Science and Technology of China, Hefei, Anhui, 230026, China.

[3] Hefei National Laboratory for Physical Sciences at the Microscale, Department of Materials Science and Engineering, Key Laboratory of Materials for Energy Conversion, Chinese Academy of Sciences (CAS), University of Science and Technology of China, Hefei, Anhui, 230026, China.

‡ Sifan Zeng and Yu Yao contributed equally to this work.

Experimental section

Synthesis of Fe_2O_3 nanoparticles. Fe_2O_3 nanoparticles were prepared by a simple precipitation method. Firstly, 25 mL of 5.4 M NaOH solution was mixed with 25 mL of 2.0 M $FeCl_3$ solution under stirring for 30 min at 80 °C. Secondly, the obtained $Fe(OH)_3$ gel was dried at 120 °C for 72 h. Subsequently, the red powders were collected, and then were washed three times with deionized water and ethanol, respectively. Finally, the Fe_2O_3 nanoparticles were obtained after drying at 60 °C for 12 h.

Synthesis of Fe@graphitic carbon structures. Fe@GC was prepared by a facile CVD method. Firstly, Fe_2O_3 nanoparticles were heated to 550 °C at a rate of 10 °C/min under Ar and H_2 atmosphere with a flow rate of 200 and 50 sccm, respectively. Secondly, C_2H_2 was pumped into the furnace with a rate of 50 sccm for 25 min. Finally, the black

products were collected without any purification after naturally cooled down. To investigate MA mechanism, Fe particles were prepared by the same process without C_2H_2. GC structures were obtained from Fe@GC after etching by 1M HCl solutions.

Materials characterization. The morphologies of the materials were investigated by Field-emission scanning electron microscopy (FESEM, FEI Apreo). The elemental composition was measured by energy-dispersive X-ray spectroscopy (EDS, Oxford instruments X-Max). Transmission Electron Microscope (JEM-2100F, JEOL, Japan) was employed to measure TEM and HRTEM. The compositions of samples were studied by the X-Ray diffraction (XRD) by a Rigaku D/max-RB12 X-Ray diffractometer with Cu Kα radiation. The Raman spectra were tested through a microscopic confocal Raman spectrometer (Renishaw RM2000) with a wavelength of 514 nm at room temperature. The magnetization properties of all samples were measured by SQUID-VSM at room temperature. The graphitic carbon content was determined by the thermogravimetry analysis (TGA). The N_2 adsorption and desorption isotherms were measured by ASAP 2020 Accelerated Surface Area and Porosimetry instrument. The electromagnetic parameters of samples mixed with wax (50 wt.%) were measured at 2 ~ 18 GHz using Vector network analyzer (N5245A, Agilent).

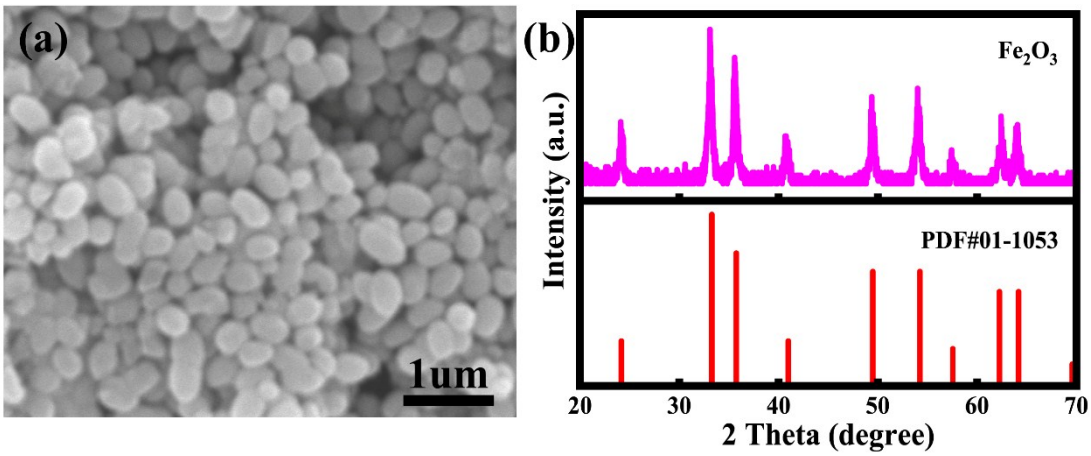

Figure S1. SEM image and XRD pattern of Fe_2O_3 particles

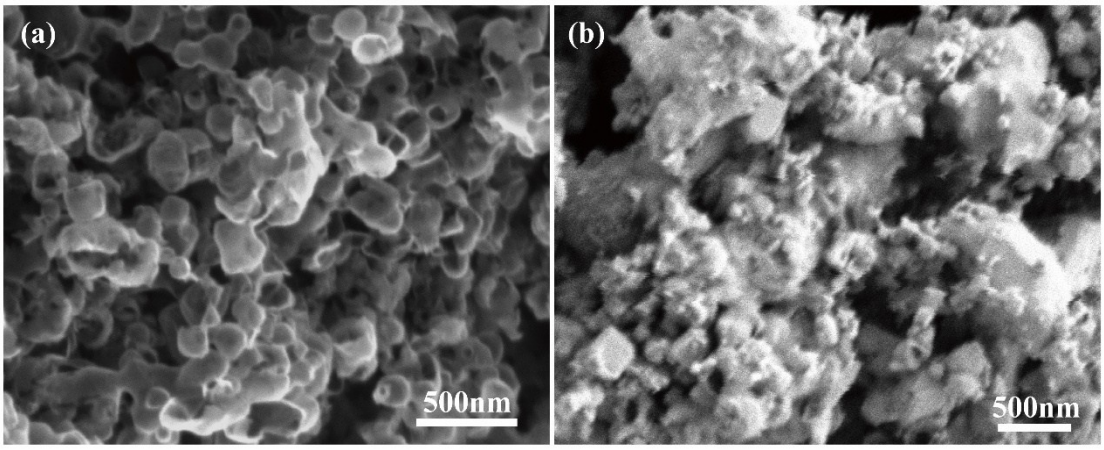

Figure S2. The SEM images of (a) GC and (b) FPs

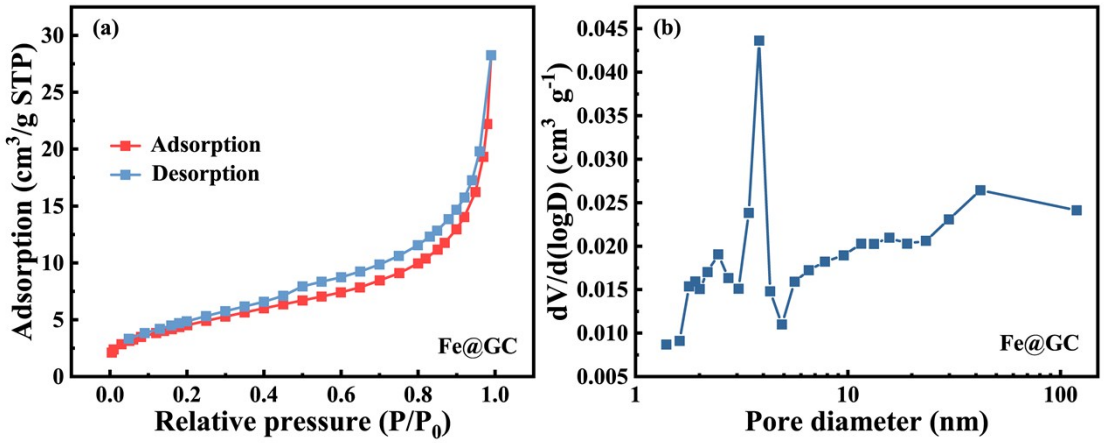

Figure S3. (a) the N_2 adsorption–desorption curves, and (d) pore size distribution of Fe@GC.

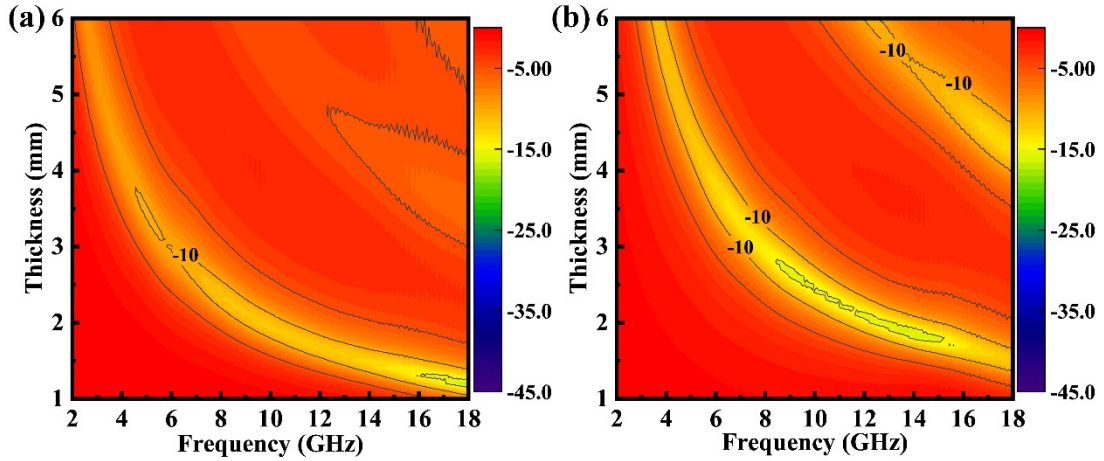

Figure S4. The reflection loss colorful mappings of (a) GC and (b) FPs.

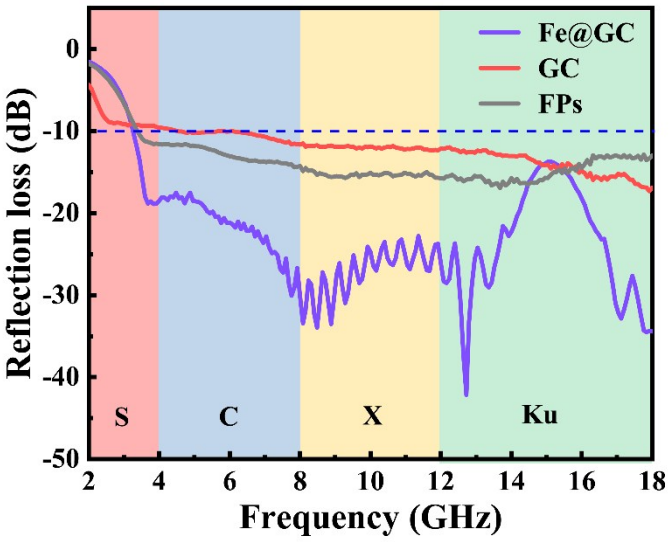

Figure S5. The curves of all RL_{min} values at every frequency of samples.

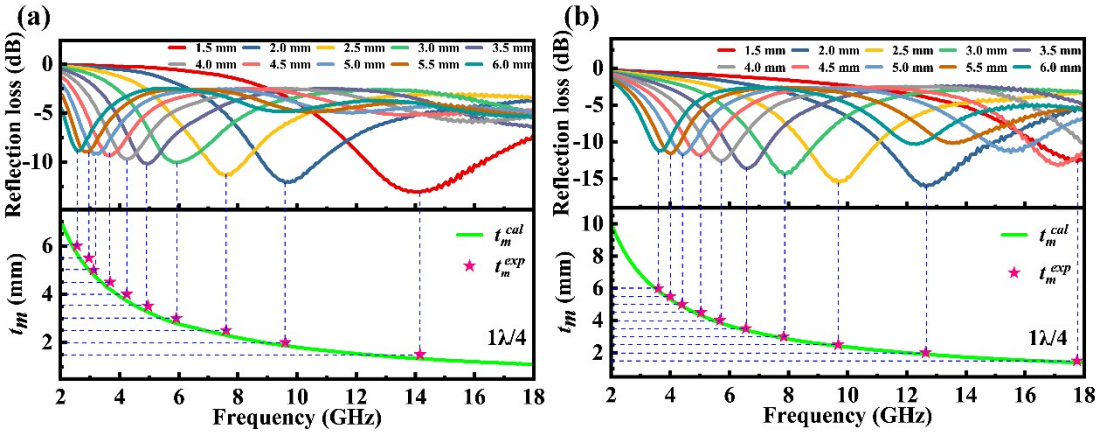

Figure S6. reflection loss curves (upper region) and dependence of matching thickness on matching frequency at the wavelength of 1/4λ (lower region) of (a) GC and (b) FPs.

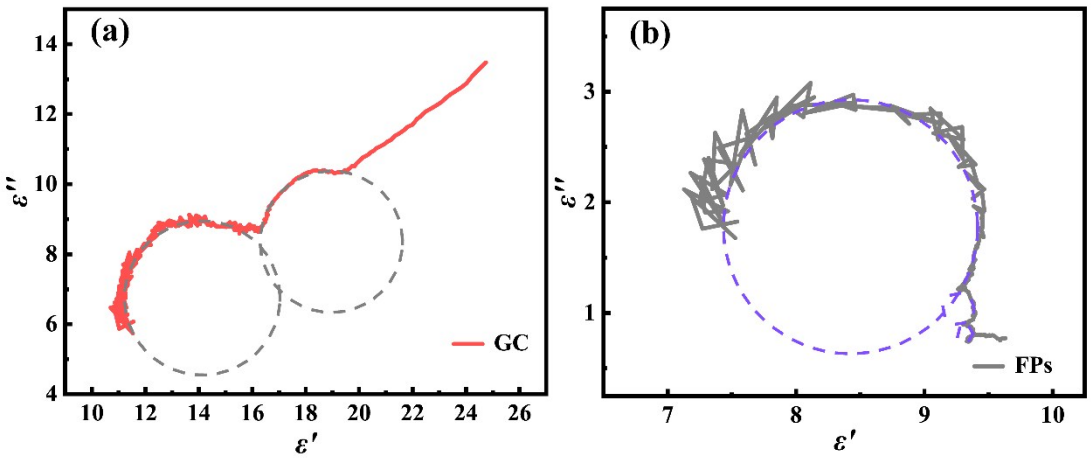

Figure S7. Cole-Cole plots of (a) GC and (b) FPs

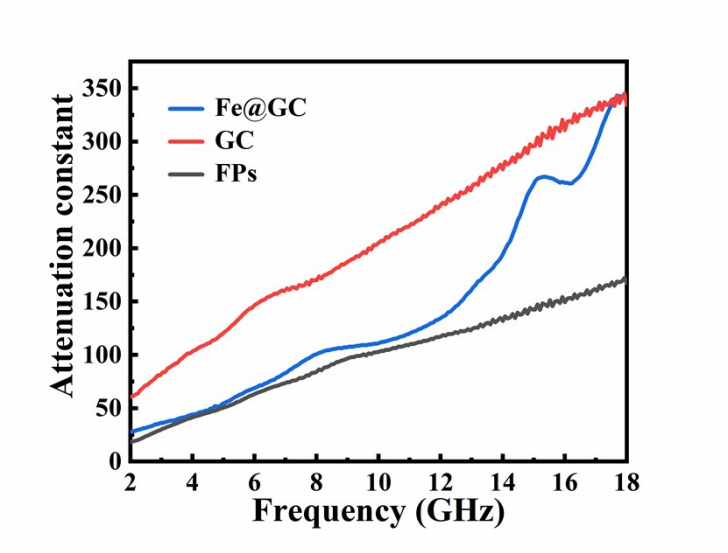

Figure S8. The attenuation constant (α) of these samples.

Equation S1:

$$\alpha = \frac{\sqrt{2}\pi f}{c} \times \sqrt{\left(\mu''\varepsilon'' - \mu'\varepsilon'\right) + \sqrt{\left(\mu''\varepsilon'' - \mu'\varepsilon'\right) + \left(\mu''\varepsilon' + \mu'\varepsilon''\right)}} \quad \text{(S1)}$$

The ε' and ε'' are real and imaginary parts of permittivity, μ' and μ'' are real and imaginary parts of permeability, f is the frequency of microwave, c is the velocity of electromagnetic wave in free space.

Table S1. Microwave absorption properties of various carbon-based materials dispersed in wax matrix in recent years

Absorbers	Mass ratio (wt. %)	Minimum RL			The widest EAB (RL ≤ -10 dB)			Ref.
		Matching thickness (mm)	RL_{min} value (dB) (Frequency, GHz)	EAB (Range, GHz)	Matching thickness (mm)	RL_{min} value (dB) (Frequency, GHz)	EAB (Range, GHz)	
Fe_3O_4/Fe@C nanorings	40	5.0	-28.18 (4.94)	~ 1.7 (3.6 - 5.3)	2.0	~ -15.0 (~14.2)	4.05 (12.80 - 16.85)	1
Fe_3O_4-Fe/Graphene Sheets	18	4.6	-58.0 (5.2)	~ 1.6 (4.5 - 6.1)	2.0	~ -31.0 (~14.0)	6.2 (11.8 - 18.0)	2
Fe/C porous nanofibers	25	4.29	-56.6 (4.96)	~ 1.3 (4.1 - 5.4)	2.0	-26.10 (11.68)	3.0 (10.5 - 13.5)	3
Graphene/Fe	20	2.5	-31.5 (14.2)	4.7 (12.4 -17.1)	2.5	-31.5 (14.2)	4.7 (12.4 - 17.1)	4
Graphene-coated Fe	40	3.0	-45.0 (7.1)	~ 2.6 (5.9 - 8.5)	2.0	~ -27.0 (~ 11. 6)	4.4 (9.7 - 14.1)	5
Porous graphene-Fe_3O_4	30	6.1	-53.0 (5.4)	~ 2.7 (4.4 - 7.1)	2.7	~ -26.0	5.4 (12.6 - 18.0)	6
Fe-Fe_3O_4@C	50	2.0	-32.9 (17.1)	~ 4.0	3.0	~ -28.0 (~ 11.0)	4.1 (9.0 - 13.1)	7
FeCo alloy/carbon	40	2.0	-33.0 (10.3)	3.3 (8.8 - 12.1)	2.0	-33.0 (10.3)	3.3 (8.8 - 12.1)	8
CoS_2/rGO	50	2.2	-56.9 (10.9)	4.1 (9.1 - 13.2)	2.2	-56.9 (10.9)	4.1 (9.1 - 13.2)	9
Ni/C nanocomposites	30	2.0	~ -19.0 (~ 11.0)	~3.2 (9.6 - 12.8)	1.5	-17.6 (~ 15.1)	4.8 (13.2 - 18.0)	10
C@$NiCo_2O_4$@Fe_3O_4	60	3.4	-43.0 (13.4)	2.1 (12.8 - 14.9)	3.4	-43.0 (13.4)	2.1 (12.8 - 14.9)	11
Mesoporous carbon	20	3.2	-50.9 (~ 11.1)	5.4 (9.1 - 14.5)	2.8	~ -26.0 (~ 11.5)	6.4 (10.6 - 17.0)	12
Hollow carbon sphere	20	2.5	~ -35.0	~3.0	1.5	-23.0	4.4 (11.5 - 15.9)	13
Yolk-shell C@C	50	1.85	-39.4 (16.48)	-	2.0	-34.8 (15.0)	5.4 (12.6 - 18.0)	14
Fe@GC	50	2.0	-42.17 (12.72)	6.72 (11.28 - 18.00)	2.0	-42.17 (12.72)	6.72 (11.28 - 18.00)	Herein

"-" denotes that it's unclear.

References

[1] Liu Y, Li Y, Jiang K, et al. Controllable synthesis of elliptical Fe_3O_4@C and Fe_3O_4/Fe@C nanorings for plasmon resonance-enhanced microwave absorption[J]. Journal of Materials Chemistry C, 2016, 4(30): 7316-7323.

[2] Qu B, Zhu C, Li C, et al. Coupling hollow Fe_3O_4-Fe nanoparticles with graphene sheets for high-performance electromagnetic wave absorbing material[J]. ACS applied materials & interfaces, 2016, 8(6): 3730-3735.

[3] Wang F, Sun Y, Li D, et al. Microwave absorption properties of 3D cross-linked Fe/C porous nanofibers prepared by electrospinning[J]. Carbon, 2018, 134: 264-273.

[4] Chen Y, Lei Z, Wu H, et al. Electromagnetic absorption properties of graphene/Fe nanocomposites[J]. Materials Research Bulletin, 2013, 48(9): 3362-3366.

[5] Zhao X, Zhang Z, Wang L, et al. Excellent microwave absorption property of graphene-coated Fe nanocomposites[J]. Scientific reports, 2013, 3: 3421.

[6] Zheng Y, Wang X, Wei S, et al. Fabrication of porous graphene-Fe_3O_4 hybrid composites with outstanding microwave absorption performance[J]. Composites Part A: Applied Science and Manufacturing, 2017, 95: 237-247.

[7] Jian X, Xiao X, Deng L, et al. Heterostructured Nanorings of Fe-Fe_3O_4@ C Hybrid with Enhanced Microwave Absorption Performance[J]. ACS applied materials & interfaces, 2018, 10(11): 9369-9378.

[8] Liu D, Qiang R, Du Y, et al. Prussian blue analogues derived magnetic FeCo alloy/carbon composites with tunable chemical composition and enhanced microwave absorption[J]. Journal of colloid and interface science, 2018, 514: 10-20.

[9] Zhang C, Wang B, Xiang J, et al. Microwave absorption properties of CoS2 nanocrystals embedded into reduced graphene oxide[J]. ACS applied materials & interfaces, 2017, 9(34): 28868-28875.

[10] Guo Z, Xie P, Dang F, et al. Bio-gel Derived Nickel/Carbon Nanocomposites with Enhanced Microwave Absorption[J]. Journal of Materials Chemistry C, 2018.

[11] Wei S, Wang X, Zhang B, et al. Preparation of hierarchical core-shell C@ NiCo2O4@ Fe3O4 composites for enhanced microwave absorption performance[J]. Chemical Engineering Journal, 2017, 314: 477-487.

[12] Cheng Y, Li Z, Li Y, et al. Rationally regulating complex dielectric parameters of mesoporous carbon hollow spheres to carry out efficient microwave absorption[J]. Carbon, 2018, 127: 643-652.
[13] Li D P, Sun Y C, Wang X, et al. Development of a hollow carbon sphere absorber displaying the multiple-reflection effect to attenuate electromagnetic waves[J]. RSC Advances, 2017, 7(60): 37983-37989.
[14] Qiang R, Du Y, Wang Y, et al. Rational design of yolk-shell C@C microspheres for the effective enhancement in microwave absorption[J]. Carbon, 2016, 98: 599-606.